DOA Estimation for Unequal Power Sources using Extremely Low Profile Aperture Coupled Microstrip Antenna

Yong Han [1], Qingyuan Fang [*2], Lizhong Song [1], Fenggang Yan [1], Xiaolin Qiao [1], and Shanna Zhuang [2]

[1] School of Electronics and Information Engineering
Harbin Institute of Technology, Weihai, 264209, China

[2] School of Information Science and Technology
Shijiazhuang Tiedao University, Shijiazhuang, 050043, China
fangqingyuanHIT@gmail.com

Abstract **─** In this paper, an aperture coupled microstrip antenna with extremely low profile ($0.022\lambda_c$, λ_c is the wavelength of the center frequency) is proposed and then applied to direction of arrival (DOA) estimation for unequal power sources. Two serial coupling slots resonating at connected frequencies are employed to expand the bandwidth of this microstrip antenna with extremely low profile. Compared with the microstrip antenna fed by a single coupling slot, the bandwidth is increased to 1.37% by using two serial coupling slots. Measurements of the antenna prototype exhibit 6.63% bandwidth ($S_{11} < -10$ dB) and agree well with the simulation results. The measured antenna gain is 5.79 dBi, and the 3 dB beam width is 56° and 112° in the E-plane and H-plane, respectively. In addition, the cross-polarization level of the prototype is −20 dB down from the co-polarization. Finally, the proposed antenna is applied in the DOA estimation for unequal power sources. Simulation results confirmed that the proposed antenna is effective and can be used in passive radar application.

Index Terms **─** Aperture coupled antenna, DOA estimation, H-shaped coupling slot, low profile, passive radar, unequal power sources.

I. INTRODUCTION

Aperture coupled microstrip antennas are extensively used for target estimation, localization, and recognition in radar systems because of their compact structure and low cost [1, 2]. With the growing demands for multi-tasking in the radar system, the space for each electronic device is strictly restricted, including the antenna. However, the compressed space will seriously limit the bandwidth of microstrip antennas, especially for the aperture coupled microstrip antenna, which is sensitive to the profile height [3-5].

For microstrip antennas, various methods have been proposed to achieve wide bandwidth. For example, a thick substrate with low permittivity is applied to expand the bandwidth; however, a thicker substrate suffers from decreased efficiency due to surface wave generation [6]. By employing diverse apertures [7] on the radiating patches, such as quasi-ring aperture [8], E-shaped aperture [9], and U-shaped aperture [10], the bandwidth can be improved. Generally, an aperture-loading technique is applied to probe feed microstrip antenna and will cause decreasing of the front-to-back (F/B) ratio for aperture coupled microstrip antennas [8]. The parasitic [11, 12] and stacked patches [13, 14] resonating at connected frequencies are applied to increase the bandwidth of the aperture coupled microstrip antennas. However, the parasitic and stacked patches will increase the antenna size or height, and such increase is undesirable for electronic devices with very limited space. To decrease the profile, artificial magnetic conductor (AMC) and electromagnetic bandgap (EBG) structures are exploited [15, 16] in the design of microstrip antennas. However, excessive parameters of AMC and EBG structures increase the design complexity and cost of antennas. Hence, concise bandwidth-enhancement methods for aperture coupled microstrip antennas with extremely low profile remain to be investigated.

Antennas working as electromagnetic wave sensors play an important role in subsequent signal processing, such as DOA estimation. Aperture coupled microstrip antennas have been widely used in DOA estimations [17-19]. DOA estimation methods based on array signal processing have been highly developed in the past three decades. One class of method, called subspace method, is very representative, in which the multiple signal classification (MUSIC) is intensively studied for its good performance in resolving adjacent sources [20-22]. However, the performance of the MUSIC method suffers

Submitted On: September 30, 2015
Accepted On: July 4, 2016

from great degradation when confronted with unequal power sources [23, 24]. Moreover, in most DOA estimation literature, the performances of proposed DOA methods for unequal power sources are seldom discussed. Actually, the sources with different power levels are very common in electronic warfare environment. For example, the powers of targets and decoys are usually different, whereas sources with equal power levels seldom exist. Hence, the performance discussion of DOA methods for unequal power sources based on aperture coupled microstrip antennas is of great significance for passive radar.

In this work, two serial H-shaped slots are exploited to expand the bandwidth of a microstrip antenna with extremely low profile (0.022λc). The bandwidth is effectively expanded without increasing the antenna profile or fabrication complexity. In addition, the H-shaped coupling slots can move the resonant frequency to a lower band, which is useful in antenna miniaturization. The measurements of the antenna prototype are in good agreement with the simulation results, which exhibit 6.63% bandwidth (from 1.415 GHz to 1.512 GHz), stable antenna gain, broad beam width, and low cross-polarization level. To investigate the performance of the proposed antenna on DOA estimation for unequal power sources, a subspace method that utilizes the noise subspace eigenvalues to estimate the DOAs of unequal power sources [25] is applied to the proposed antenna. The simulation results demonstrate that the proposed antenna can be used for DOA estimation with unequal power sources and show better performance when applied as a method in [25] than the MUSIC method.

II. ANTENNA CONFIGURATION

As shown in Fig. 1, the proposed antenna is a 2 × 1 array (87 mm apart from each other) consisting of two square radiating patches etched on layer A (Rogers 4003C substrate with relative permittivity of 4.5 and thickness 0.508 mm) and a ground plane etched on layer C (Rogers 5880 substrate with relative permittivity of 2.2 and thickness 0.508 mm).

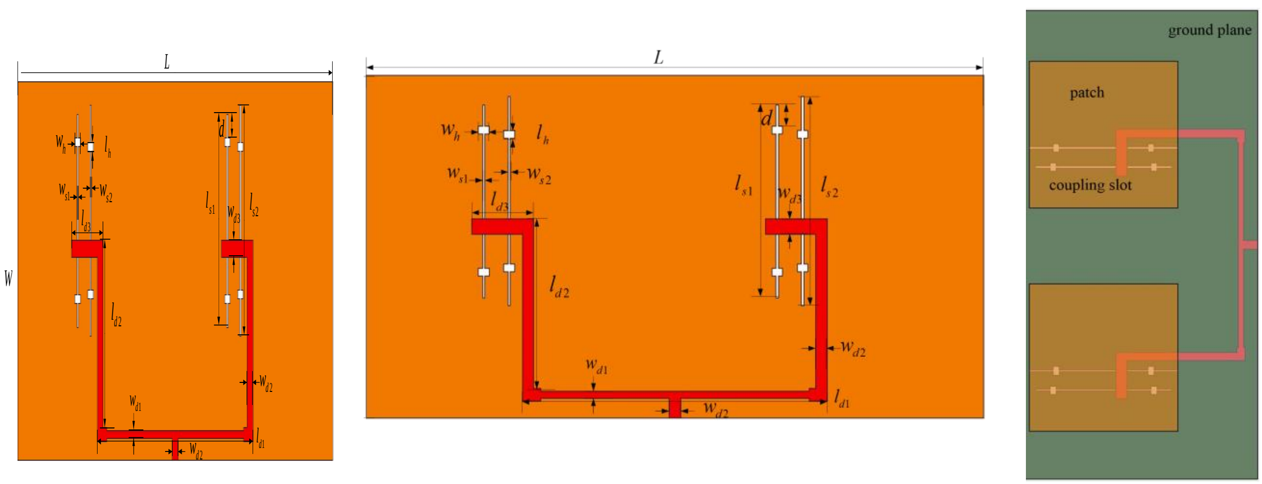

(a) (b) (c)

Fig. 1. Antenna array geometry with key parameters: (a) Side view, (b) ground plane and power divider, and (c) cross views.

Between the radiating patches and the ground plane is an air space (Layer B) with relative dielectric constant 1 and thickness of 4.5 mm (0.022λ_c). The length of the square radiating patches printed on the bottom side of layer A is 53.20 mm. Two serial H-shaped coupling slots are embedded in the ground plane at the bottom side of layer C. The coupling slots with slightly different lengths resonating at connected working frequencies are exploited to expand the bandwidth of the antenna. The parameters of proposed antenna are optimized by Ansoft HFSS. The final parameters of the proposed antenna are listed in Table 1.

Table 1: Antenna parameters

Parameter	Value (mm)	Parameter	Value (mm)
W	87.00	L	170.00
w_{d1}	2.45	l_{d1}	83.90
w_{d2}	3.13	l_{d2}	43.11
w_{d3}	4.00	l_{d3}	17.00
w_{s1}	0.68	l_{s1}	49.00
w_{s2}	0.70	l_{s2}	53.00
w_h	1.16	l_h	2.00
d	7.50		

III. SIMULATED AND MEASURED RESULTS AND DISCUSSION

The thickness of the air layer is 4.5 mm, which is extremely low ($0.022\lambda_c$@1.46GHz) and will seriously affect the bandwidth of the microstrip antenna. The coaxial probe fed microstrip antennas with such ultralow profile are studied in [7, 10, 26, 27]. In [7], the multi-couple staggered slots on the patch produce a 3.9% bandwidth with substrate thickness of $0.022\lambda_c$. In [26], an E-shaped microstrip patch antenna illustrates a 15.2% bandwidth with a low profile of $0.0583\lambda_c$. In [27], and [28], the U-slot microstrip antennas show 11.3% and 20%–30% bandwidth with $0.0581\lambda_c$ and $0.08\lambda_c$ profiles, respectively. However, little research has been conducted on the aperture coupled microstrip antenna with extremely low profile. In the present work, an effective and concise method employing two H-shaped coupling slots is studied.

A. Bandwidth comparison between antennas with different numbers of coupling slots

The configurations of aperture coupled microstrip antennas with one, two, and three coupling slots are shown in Fig. 2. In Fig. 2 (a), the length of feed line (l_{d3}) is 14 mm, and the length of coupling slot (l_{s2}) is 56 mm, which is optimized to match with the feed network. In Fig. 2 (b), the length of the middle slot is 51 mm, and other parameters are the same as those of the antenna shown in Fig. 1.

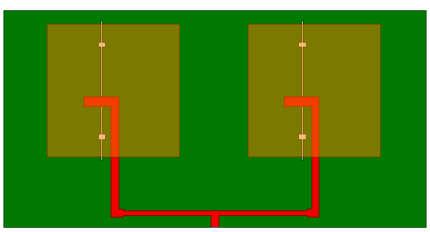

(a)

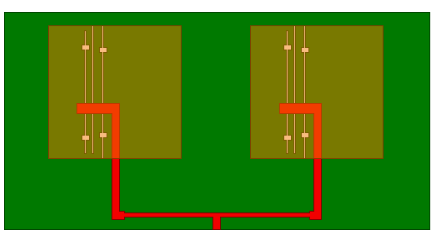

(b)

Fig. 2. Aperture coupled microstrip antennas with different coupling slots: (a) one coupling slot and (b) three coupling slots.

The simulated results of reflection coefficient (S_{11}) for antennas with different numbers of coupling slots are shown in Fig. 3, in which the bandwidths of antennas with one, two, and three coupling slots are 3.76% (from 1.434 GHz to 1.489 GHz), 5.13% (from 1.424 GHz to 1.499 GHz), and 5.54% (from 1.386 GHz to 1.465 GHz), respectively. Notably, the impendence bandwidth increased to 36.4% by utilizing two serial coupling slots compared with one coupling slot.

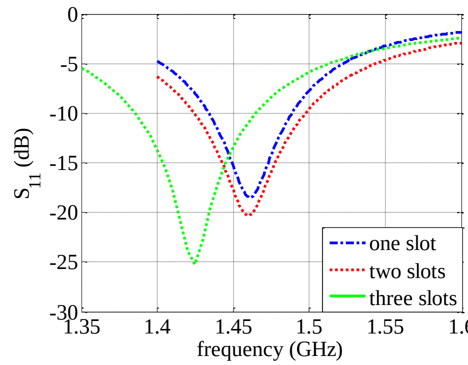

Fig. 3. Simulated S_{11} of antennas with different numbers of coupling slots.

The amplitudes of the surface current distributions at different frequencies on the ground plane are shown in Fig. 4. As shown in Fig. 4 (a), the longer coupling slot is excited more strongly than the shorter coupling slot. This finding indicates that the performance of the antenna at 1.43 GHz (lower working frequency) is mainly determined by the longer coupling slot. As shown in Fig. 4 (b), the shorter slot is excited at 1.5 GHz. However, only one longer coupling slot is available in Fig. 4 (c). Therefore, the working bandwidth will be narrower than that of the antenna with two resonant coupling slots.

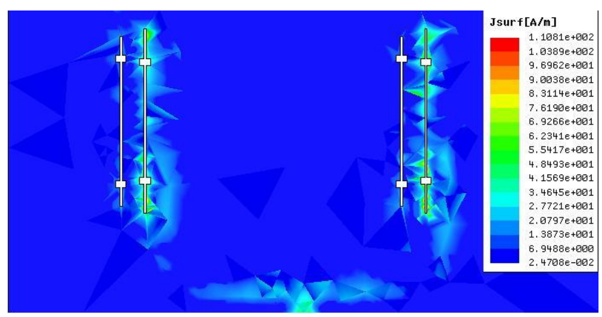

(a)

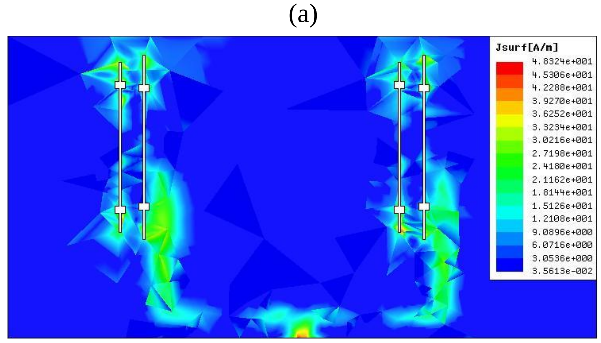

(b)

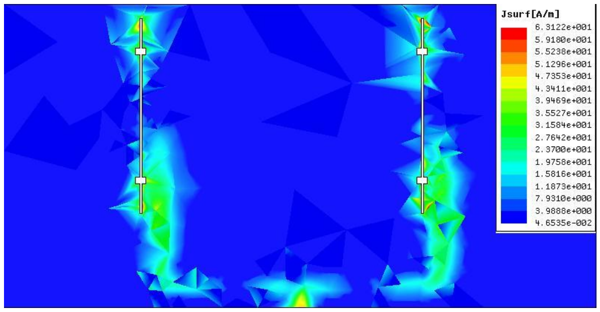

(c)

Fig. 4. Surface current distributions: (a) antenna with two coupling slots at 1.43 GHz, (b) antenna with two coupling slots at 1.5 GHz, and (c) antenna with one coupling slot at 1.5 GHz.

Consequently, an additional serial slot can enhance the working bandwidth of an aperture coupled microstrip antenna, which can also be applied to other aperture coupled antenna designs. Notably, the coupling slots on the ground plane will deteriorate the F/B ratio; thus, a trade-off between the bandwidth and the F/B ratio should be made. In this work, a configuration with two coupling slots is studied and fabricated.

B. Parametric study

Parameters with critical influence on the performance of the proposed antenna are studied. The effects on working frequency introduced by the length of coupling slots (l_{s1} and l_{s2}) are shown in Fig. 5. It is noted that the working frequency is sensitive to the length of coupling slots. Extending l_{s1} will shift the working frequency to a lower band, so does the same of l_{s2}. Comparison of Fig. 5 (a) and Fig. 5 (b) shows that the longer coupling slot exerts a dominant effect in determining the working frequency. Simulation results of S_{11} at different widths of the coupling slot are shown in Fig. 6. The width of coupling slots can slightly influence the resonant frequency; however, this width also influences the impendence matching.

In the proposed antenna, the optimization results of w_{s1} and w_{s2} are 0.68 and 0.70 mm, correspondingly.

The effects of tiny slot parameters, such as length l_h, width w_h, and the position of the tiny slot on the antenna performance are shown in Fig. 7. As illustrated in Figs. 7 (a) and 7 (b), increasing the slot width and length will move the working frequency to the lower band. Compared with the slot length l_h, the antenna is more easily influenced by the slot width w_h.

The influence of tiny slot position on the antenna performance is presented in Fig. 8. The distance of the tiny slot from the top of the long slot is denoted by d. From Fig. 8, we can conclude that the position of the tiny slot also affects the working frequency of the antenna. The operation frequency increases as the tiny slot moves far away from the long slot center.

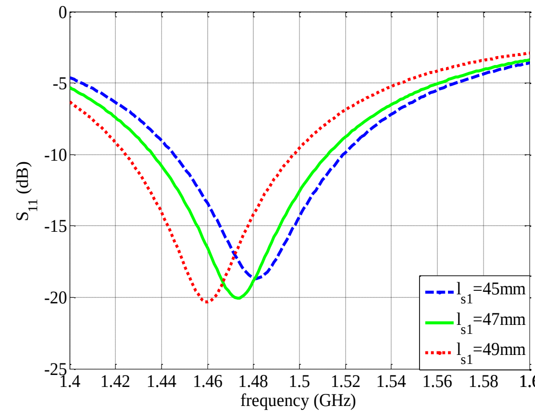

(a)

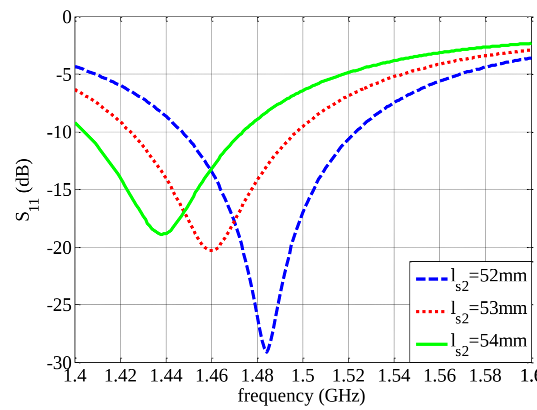

(b)

Fig. 5. Simulated S_{11} with different lengths of coupling slots: (a) simulated S_{11} under l_{s2} = 53 mm, and (b) simulated S_{11} under l_{s1} = 49 mm.

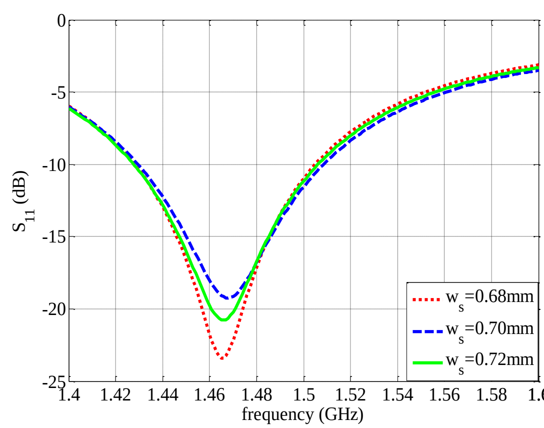

Fig. 6. Simulated S_{11} with different coupling slot widths.

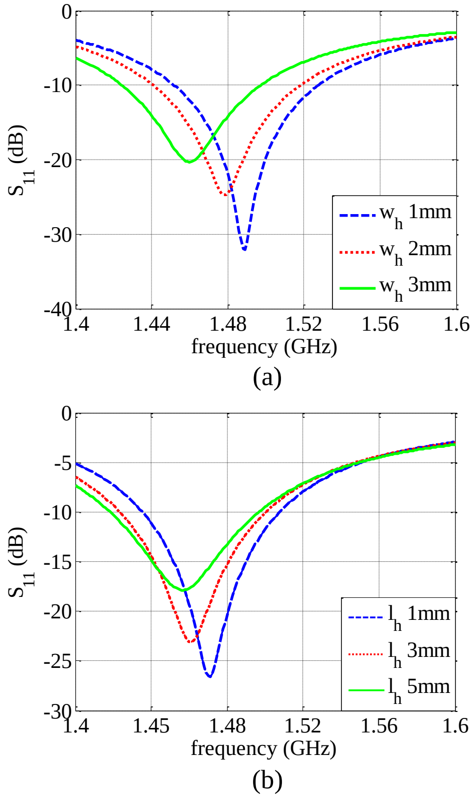

Fig. 7. Simulated S_{11} with different parameters of tiny slot perpendicular to the long coupling slot: (a) with different w_h and (b) with different l_h.

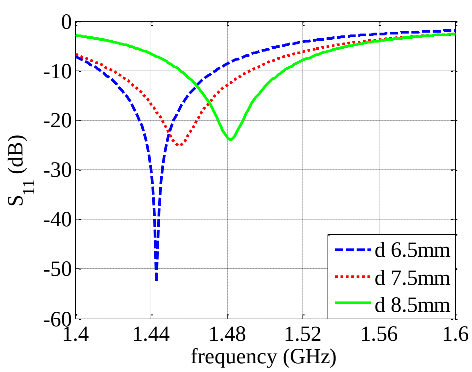

Fig. 8. Simulated S_{11} with different tiny slot positions.

The normalized input impedance as a function of w_h and l_h is shown in Fig. 9. The working frequency is decreased when w_h and l_h are increased. As shown in Fig. 9, increasing the w_h and l_h also increases the normalized input resistance and reactance. Simultaneously, the resonant frequency is shifted to the lower band.

After the parametric studies, the effects of coupling slots on the performance of antenna are clearly understood and can be referred to when we design other aperture coupled microstrip antennas. The tiny slots play an important role in determining the working frequency of the proposed antenna. Simulated results of S_{11} when employing H-shaped coupling slots (with tiny slots) and conventional slots (without tiny slots) are shown in Fig. 10; the resonant frequency of the proposed antenna is shifted to a lower frequency band when the H-shaped coupling slots are employed compared with conventional coupling slots.

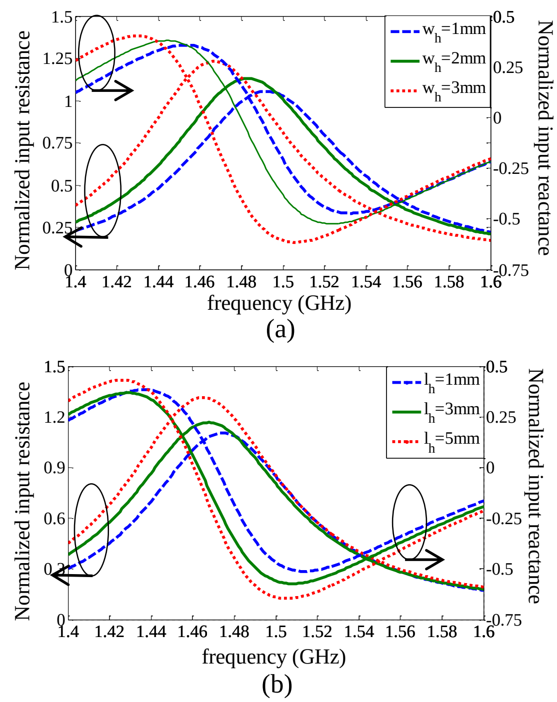

Fig. 9. Normalized input impedance of the proposed antenna: (a) with different w_h and (b) with different l_h.

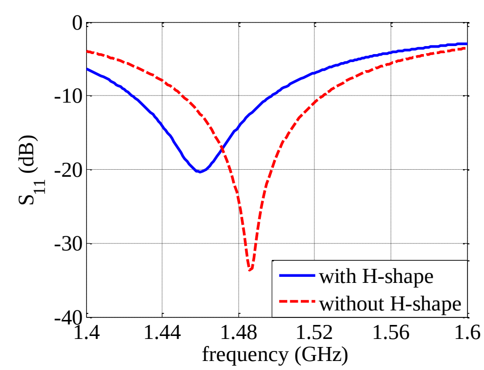

Fig. 10. Simulated S_{11} with H-shaped coupling slots and conventional coupling slots.

C. Experimental results

As shown in Fig. 11, a prototype of the proposed antenna with an overall size of $0.83\lambda_c \times 0.43\lambda_c \times 0.022\lambda_c$ is fabricated and measured with an Agilent E8363B vector network analyzer. The measured S_{11} is shown in Fig. 12, which illustrates a bandwidth of 6.63% (from 1.415 GHz to 1.512 GHz) as $S_{11} < -10$ dB and agrees well with the simulation result.

The simulated and measured antenna gain (Table 2) presents the same tendency as the frequency varies from low to high. The measured antenna gain is lower than the simulation results, which may be caused by the loss of substrate and fabrication errors. The gain of the proposed antenna is not as high as the traditional microstrip antenna because of the apertures in the ground plane leading to back radiation.

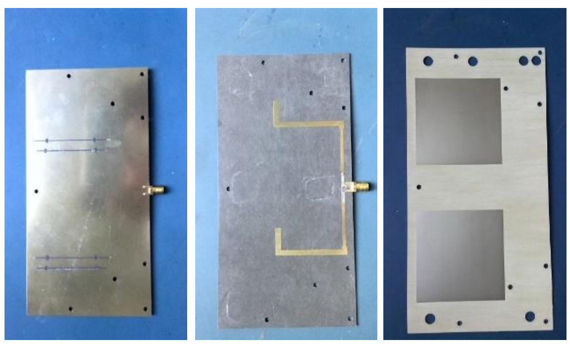

(a) (b) (c)

Fig. 11. Antenna prototype: (a) the ground plane with coupling slots, (b) the feed network, and (c) the radiating patches.

Table 2: Antenna gain

Frequency (GHz)	Simulated Gain (dB)	Measured Gain (dB)
1.42	6.02	4.37
1.45	6.25	5.32
1.48	6.47	5.39
1.51	6.70	5.79

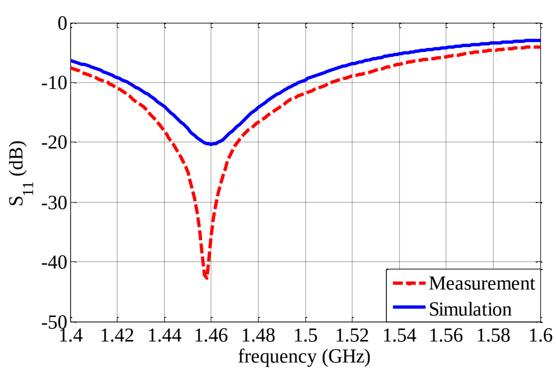

Fig. 12. Measured and simulated results of S_{11} as a function of frequency.

The normalized radiation patterns at 1.45 GHz are measured in both principal planes and are shown in Fig. 13. The half-power beam width (HPBW) of the proposed antenna is 56° and 112° in the E-plane and H-plane, respectively. The measured and simulated radiation patterns show good agreement with each other. The cross-polarization level is approximately −20 dB down from the co-polarization on boresight in both E-plane and H-plane. The F/B ratio is not very high at approximately 10 dB. This can be attributed to the coupling slots in the ground plane leading to the leakage of the electromagnetic wave.

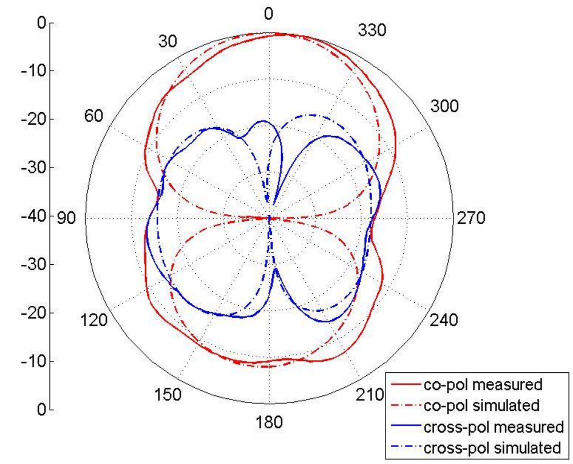

(a)

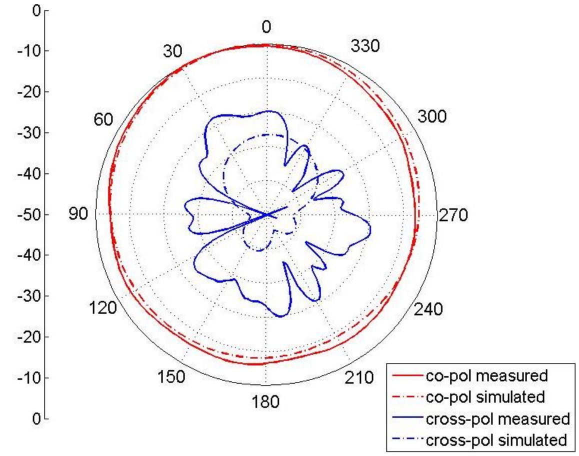

(b)

Fig. 13. Measured and simulated results of normalized co-polarized and cross-polarized radiation patterns at 1.45 GHz: (a) in xoy plane (E-plane) and (b) in yoz plane (H-plane).

IV. DOA ESTIMATION EXPERIMENT FOR UNEQUAL POWER SOURCES

Aperture coupled microstrip antennas used for DOA estimation are extensively studied [17-19]. DOA estimation is the first step for target detection in passive radar application and can provide target direction to passive radar for target tracking until the target is destroyed. The performance of microstrip antennas when applied in DOA estimation has been investigated extensively by employing the MUSIC method [22, 28]. In those studies, the DOA estimation for sources (targets) with equal power levels is intensively investigated. However, the performance of DOA estimation for unequal power sources when employing microstrip antennas as the receiving antenna array is seldom conducted. Sources with unequal power levels are commonly observed in practical applications, especially in passive radar. In electronic warfare environment, multiple targets exhibit different power levels. For example, decoys are usually disposed around the real target (usually the active radar) to protect it from being attacked. In this case, the decoys and the real target transmit unequal power signals that reach the receiving antenna array of passive radar simultaneously. Therefore, the received signals often present unequal power levels for passive radar. However, the performance of the MUSIC method suffers from great degradation when resolving the unequal power sources. Once the DOA estimation of the target becomes inaccurate, the following target location, recognition, and tracking will deteriorate sharply. In this work, another subspace method [25] is applied to DOA estimation for unequal power sources based on the proposed antenna. Simultaneously, the performance of the MUSIC method for unequal power sources based on the proposed antenna is also simulated to make comparisons with the method in [25].

In [25], the invariance property of the noise subspace (IPNS) is proposed when the powers of the sources are increased. We call the method proposed in [25] as the IPNS method. The invariant noise subspace eigenvalues are then used to estimate the DOAs of the sources. The uniform linear antenna array configuration used for DOA estimation is shown in Fig. 14.

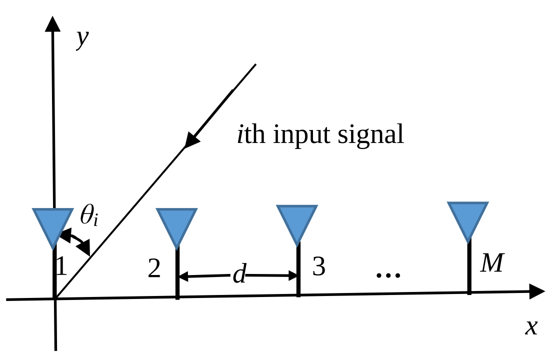

Fig. 14. Configuration of uniform linear array.

The number of antenna element is M, and the distance between each element is d. The total number of input signals is P. The DOA of the ith input signal is θ_i.

The covariance matrix of the antenna array output $\mathbf{R}$ can be replaced by a maximum likelihood estimate $\hat{\mathbf{R}}$ expressed as:

$$\hat{\mathbf{R}} = 1/L\sum_{j=1}^{L}\mathbf{X}(t_j)\mathbf{X}(t_j)^{\mathrm{H}}, \qquad (1)$$

where $\mathbf{X}(t)=[x_1(t)\cdots x_M(t)]^{\mathrm{T}}$ is the array signal vector, L is the number of snapshots, $(\bullet)^{\mathrm{H}}$ and $(\bullet)^{\mathrm{T}}$ denote the conjugate transpose and the transpose, respectively. The noise subspace eigenvalues $\lambda_i, i = P+1, P+2,\cdots M$ can be obtained through the eigenvalue decomposition (EVD) of $\mathbf{R}$. In the IPNS method, another covariance matrix is constructed as follows:

$$\mathbf{D} = \mathbf{R} + h\mathbf{a}(\theta)\mathbf{a}(\theta)^{\mathrm{H}}, \qquad (2)$$

where $\mathbf{a}(\theta)$ is the steering vector of the receiving antenna array. In [25], the noise subspace eigenvalues of $\mathbf{D}$ have been proven to remain the same as $\mathbf{R}$ when only the power of the input signals increased. This invariance property of the noise subspace can be used for DOA estimation. Therefore, the spatial spectrum obtained from the IPNS method is given as

$$P(\theta) = \frac{1}{\sum_{i=P+1}^{M}(\hat{\mu}_i - \hat{\lambda}_i)}, \qquad (3)$$

where $\hat{\mu}_i$ and $\hat{\lambda}_i$ are the noise subspace eigenvalues of the sample covariance matrix $\hat{\mathbf{D}}$ and $\hat{\mathbf{R}}$, respectively. The sample covariance matrix $\hat{\mathbf{D}}$ is obtained through $\hat{\mathbf{D}} = \hat{\mathbf{R}} + h\mathbf{a}(\theta)\mathbf{a}(\theta)^{\mathrm{H}}$, where $h = \mathrm{tr}(\hat{\boldsymbol{R}})/M$ and $\mathrm{tr}(\hat{\boldsymbol{R}})$ denote the trace of $\hat{\mathbf{R}}$. The DOAs of the sources are the P maxima of $P(\theta)$.

A uniform linear array comprising five proposed antennas is used to estimate the DOAs of the unequal power sources. The coupling between the antennas is not considered to assess the influence of unequal power levels on the spatial spectrums. Assuming that the strong signal (signal to noise ratio, SNR 25 dB) impinges from −6° and −3°, the weak signal (SNR 5 dB) impinges from 6° and 3°. The spatial spectrums of the MUSIC method and IPNS method when employing the measured and simulated antenna radiation patterns are shown in Figs. 15 (a) and 14 (b).

As shown in Fig. 15, the proposed antenna can be used to perform DOA estimation for unequal power sources; the DOA estimation methods also showed almost the same performance when using the simulated and measured antenna radiation patterns. This finding indicates that the measured radiation pattern of the proposed antenna is in good agreement with the simulation results. Comparison of Figs. 15 (a) and 15 (b) shows that the MUSIC method is insufficient, whereas the IPNS method is valid in resolving the adjacent unequal power sources. The capability of DOA methods in distinguishing the adjacent sources will directly affect their performance when they are applied in engineering applications. The experiment demonstrates that the proposed antenna can be applied to perform DOA estimation for unequal power sources. Sources with unequal powers are commonly observed in an electronic warfare environment. The received signals usually present unequal power levels, especially for passive radar application. The real active radar and decoys of the enemy used as jamming to protect the active radar demonstrate different power levels. The signals with unequal powers transmitted from the active radar and decoys reach the antenna array of the passive radar simultaneously. As shown in Fig. 15, the IPNS method is more efficient in resolving the adjacent sources than the MUSIC method, especially for unequal power sources, when the proposed antenna is used as the receiving antenna array element. Therefore, the IPNS method based on the proposed antenna is more capable in resolving the adjacent real targets and decoys, which are significant for passive radar in anti-jamming application.

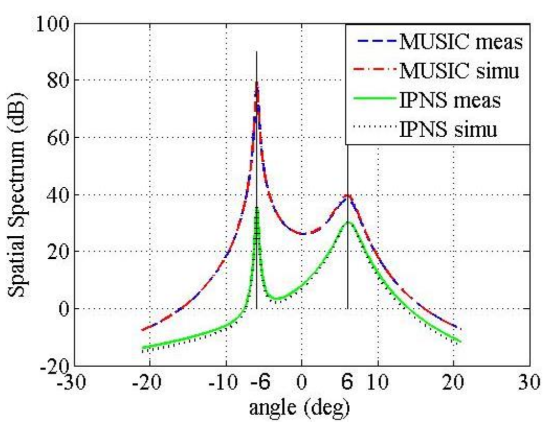

(a)

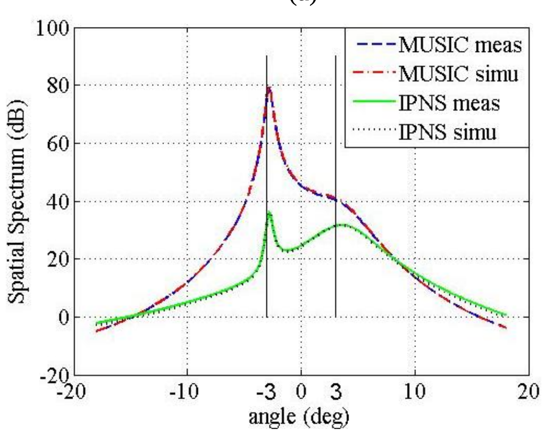

(b)

Fig. 15. Spatial spectra of different methods using the measured and simulated antenna radiation patterns: (a) large angle separation, and (b) small angle separation.

V. CONCLUSION

A serial H-shaped aperture coupled microstrip antenna with extremely low profile is investigated and applied in DOA estimation for unequal power sources. The proposed antenna exhibits a bandwidth of 6.63% (from 1.415 GHz to 1.512 GHz) and increases 1.37% bandwidth compared with one coupling slot aperture coupled antenna. Good radiation patterns and low cross-polarization level are also available. The serial coupling slots, which does not increase the design and manufacture complexity, is demonstrated to comprise an effective method to expand the bandwidth of the aperture coupled microstrip antenna. Moreover, the proposed antenna proved to be valid in the DOA estimation for unequal power sources, which is useful in passive radar to estimate the target and decoys.

ACKNOWLEDGMENT

This work was supported by the Natural Science Foundation of China (Grant No. 61571154), Natural Science Foundation of Hebei Province (No. F2014210123), Natural Scientific Research Innovation Foundation in Harbin Institute of Technology (HIT.NSRIF 2013130), Shandong Provincial Natural Science Foundation (ZR2014FQ003), China Postdoctoral Science Foundation (2015M571414), and the Fundamental Research Funds for the Central Universities (HIT.NSRIF.2016102).

REFERENCES

[1] S. Gao, L. W. Li, M. S. Leong, and T. S. Yeo, "A broad-band dual-polarized microstrip patch antenna with aperture coupling," *IEEE Trans. Antennas Propagat*., vol. 51, no. 4, pp. 898-900, 2003.

[2] C. J. Meagher and S. K. Sharma, "A wideband aperture-coupled microstrip patch antenna employing spaced dielectric cover for enhanced gain performance," *IEEE Trans. Antennas Propagat*., vol. 58, no. 9, pp. 2802-2810, 2010.

[3] F. Yang, X. X. Zhang, X. Ye, and Y Rahmat-Samii, "Wide-band E-shaped patch antennas for wireless communications," *IEEE Trans. Antennas Propagat*., vol.49, no. 7, pp. 1094-1100, 2001.

[4] H. S. Shin and N. Kim. "Wideband and high-gain one-patch microstrip antenna coupled with H-shaped aperture," *Electron. Lett.*, vol.38, no.19, pp. 1072-1073, 2002.

[5] K. L. Wong, H. C. Tung, and T. W. Chiou, "Broadband dual-polarized aperture-coupled patch antennas with modified H-shaped coupling slots," *IEEE Trans. Antennas Propagat*., vol. 50, no. 2, pp. 188-191, 2002.

[6] K. F. Lee and K. F. Tong, "Microstrip patch antennas-Basic characteristics and some recent advances," *Proc. IEEE*, vol. 100, no. 7, pp. 2169-2180, 2012.

[7] S. Xiao, Z. Shao, B. Z. Wang, M. T. Zhou, and M. Fujise, "Design of low-profile microstrip antenna with enhanced bandwidth and reduced size," *IEEE Trans. Antennas Propagat*., vol. 54, no. 5, pp. 1594-1599, 2006.

[8] M. M. Honari, A. Abdipour, and G. Moradi, "Bandwidth and gain enhancement of an aperture antenna with modified ring patch," *IEEE Antennas Wireless Propag. Lett*., vol. 10, pp. 1413-1416, 2011.

[9] B. K. Ang and B. K. Chung, "A wideband E-shaped microstrip patch antenna for 5-6 GHz wireless communications," *Prog. Electromagn. Res.*, vol. 75, pp. 397-407, 2007.

[10] A. Khidre, K. F. Lee, A. Z. Elsherbeni, and F. Yang, "Wide band dual-beam U-slot microstrip antenna," *IEEE Trans. Antennas Propagat*., vol. 61, no. 3, pp. 1415-1418, 2013.

[11] T. Y. Yang, W. Hong, and Y. Zhang, "Wideband high - gain low - profile dual - polarized stacked patch antenna array with parasitic elements," *Microw. Opt. Techn. Let.*, vol. 57, no. 9, pp. 2012-2016, 2015.

[12] C. Deng, "Wideband microstrip antennas loaded by ring resonators," *IEEE Antennas Wireless Propag. Lett*., vol. 12, pp. 1665-1668, 2013.

[13] M. Barba, "A high-isolation, wideband and dual-linear polarization patch antenna," *IEEE Trans. Antennas Propagat*., vol. 56, no. 5, pp. 1472-1476, 2008.

[14] A. A. Serra, P. Nepa, G. Manara, G. Tribellini, and S. Cioci, "A wide-band dual-polarized stacked patch antenna," *IEEE Antennas Wireless Propag. Lett*., vol. 6, pp. 141-143, 2007.

[15] A. P. Feresidis, G. Goussetis, S. Wang, and J. C. Vardaxoglou, "Artificial magnetic conductor surfaces and their application to low-profile high-gain planar antennas," *IEEE Trans. Antennas Propagat*., vol. 53, no. 1, pp. 209-215, 2005.

[16] J. Liang and H. Y. D. Yang, "Radiation characteristics of a microstrip patch over an electromagnetic bandgap surface," *IEEE Trans. Antennas Propagat*., vol. 55, no. 6, pp. 1691-1697, 2007.

[17] K. Gotsis, K. Siakavara, and J. N. Sahalos, "On the direction of arrival (DoA) estimation for a switched-beam antenna system using neural networks," *IEEE Trans. Antennas Propagat*., vol. 57, no. 5, pp. 1399-1411, 2009.

[18] N. J. G. Fonseca, M. Coudyser, J. J. Laurin, and J. Brault, "On the design of a compact neural network-based DOA estimation system," *IEEE Trans. Antennas Propagat*., vol. 58, no. 2, pp. 357-366, 2010.

[19] M. Coulombe, S. F. Koodiani, and C. Caloz, "Compact elongated mushroom (EM)-EBG structure for enhancement of patch antenna array performances," *IEEE Trans. Antennas Propagat*., vol. 58, no. 4, pp. 1076-1086, 2010.

[20] R O. Schmidt. Multiple emitter location and signal parameter estimation [J], *IEEE Trans. Antennas Propagat*., vol. 34, no. 3, pp. 276-280, 1986.

[21] F. G. Yan, M. Jin, S. Liu, and X. L. Qiao, "Real-valued MUSIC for efficient direction estimation with arbitrary array geometries," *IEEE Trans. Signal Proces*., vol. 62, no. 6, pp. 1548-1560, 2014.

[22] C. H. Niow and H. T. Hui, "Improved noise modeling with mutual coupling in receiving antenna arrays for direction-of-arrival estimation," *IEEE Trans. Wireless Commu.*, vol. 11, no. 4, pp. 1616-1621, 2012.

[23] Q. Fang, Y. Han, M. Jin, and X. L. Qiao, "Joint DOA and polarization estimation for unequal power sources," *International Antenna. Propagat.*, 2015.

[24] M. L. McCloud and L. L Scharf, "A new subspace identification algorithm for high-resolution DOA estimation," *IEEE Trans. Antennas Propagat*., vol. 50, no. 10, pp. 1382-1390, 2002.

[25] A. Olfat and S. Nader-Esfahani, "A new signal subspace processing for DOA estimation," *IEEE Proc. Microwave Antenna Propagat.*, vol. 84, no. 4, pp. 721-728, 2004.

[26] B. K. Ang and B. K. Chung, "A wideband E-shaped microstrip patch antenna for 5-6 GHz wireless communications," *Prog. Electromagn. Res.*, vol. 75, pp. 397-407, 2007.

[27] K. F. Lee, K. M. Luk, K. F. Tong, S. M. Shum, T. Huynh, and R. Q. Lee, "Experimental and simulation studies of the coaxially fed U-slot rectangular patch antenna," *Proc. IEEE*, vol. 144, no. 5, pp. 354-358, 1997.

[28] M. Coulombe, S. F. Koodiani, and C. Caloz, "Compact elongated mushroom (EM)-EBG structure for enhancement of patch antenna array performances," *IEEE Trans. Antennas Propagat*., vol. 58, no.4, pp. 1076-1086, 2010.

Yong Han was born in Heilongjiang Province, China, in 1976. He received his Ph.D. degree from Harbin Institute of Technology, Harbin, China, in 2010. He is now a Lecturer in the School of Information and Electrical Engineering in Harbin Institute of Technology, Weihai, China. His research interests include array signal processing and polarization sensitive array signal processing.

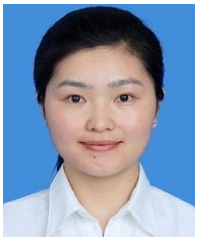

Qingyuan Fang was born in Shandong Province, China, in 1987. She received her M.S. degree and Ph.D. degree from Harbin Institute of Technology in 2010 and 2015, respectively. Now, she is a Lecturer in the School of Information Science and Technology in Shijiazhuang Tiedao University, Shijiazhuan, China. Her research interests include anti-jamming technology in passive radar and antenna technology.

Lizhong Song was born in Liaoning Province, China, in 1975. He received the Master degree and Ph.D. degree from Harbin Institute of Technology in 2001 and 2005, respectively. He is a Professor and Doctoral Supervisor of Harbin Institute of Technology at Weihai. His research interests include antenna design, wireless electromagnetic wave propagation, microwave technology and radar signal processing.

Fenggang Yan was born in ShaXi, China, in 1983. He received the B.E., M.S., and Ph.D. degrees in Information and Communication Engineering from Xi'an Jiaotong University, Xi'an, the Graduate School of Chinese Science of Academic, Beijing, and Harbin Institute of Technology (HIT), Harbin, in 2005, 2008, and 2013, respectively. Since August 2015, he has been an Associate Professor with the Department of Electronics Information Engineering, HIT, Weihai, China. His current research interests include array signal processing and statistical performance analysis

Xiaolin Qiao was born in Inner Mongolia Autonomous Region, China, in June 1948. He received the B.E., M.S., and Ph.D. degrees in Information and Communication Engineering from Harbin Institute of Technology, Harbin, China, in1976, 1983, and 1991, respectively. His research interests are in the areas of signal processing, wireless communication, special radar, parallel signal processing, and radar polarimetry.

Shanna Zhuang was born in Henan Province, China, in 1985. She received the B.Sc. degree in Electrical Information Engineering in 2007 and the Ph.D. degree in Communication and Information System in 2012 from Nanjing University of Science and Technology, Nanjing, China. She is now a Lecturer in the School of Information Science and Technology in Shijiazhuang Tiedao University, Shijiazhuang, China. Her research interests include cognitive radar and adaptive waveform design.